24th INTERNATIONAL CONGRESS ON SOUND AND VIBRATION
23–27 July 2017, London

ICSV24
23-27JULY 2017
LONDON CALLING

HEAT TRANSFER FROM A FLAT PLATE UNDER IMPINGING ACOUSTIC OSCILLATIONS

Robinson, Nick and Lawn, Chris
School of Engineering and Materials Science, Queen Mary University of London
E mail: C.J.Lawn@qmul.ac.uk

In a particular design of thermoacoustic engine for electricity generation, heat transfer to the hot end of the regenerator is through radiation from a plate heated by a fire underneath it. The travelling acoustic waves impinge on the plate and cool it substantially, thus degrading the heat transfer to the regenerator. The need to quantify this process uncovered the absence of data for heat transfer to impinging acoustic waves, and led to this experimental study. A 300mm circular duct was positioned vertically over a flat aluminium plate, which was electrically heated from below to about 58 degC by temperature-controlled pads. Two sub-woofers fed sound into the duct, and the acoustic impingement velocity was determined by extrapolating two-microphone measurements, for three frequencies: 30 Hz, 50 Hz and 90 Hz. The temperature difference between the plate and the impinging air was recorded by thermocouples, and was typically 30 degC. The heat flux distribution from the plate to the air was measured by traversing a calibrated conduction meter and the Nusselt numbers were evaluated as a function of the amplitude of the acoustic velocity and the frequency. As expected from the measurement of acoustic velocity profiles close to the plate, *Nu* increased radially from a base level on the axis of the duct to a position near the lip, and then decreased rapidly as the acoustic waves spread out into the surroundings. For given radial positions, provided the enhancement in heat transfer over the natural convection background exceeded 50%, a linear correlation of *Nu* with the ratio of stroke length to thermal penetration depth was found. Enhancements in heat transfer by up to a factor of five were recorded. However, suppression of the natural convection was observed when the stroke lengths were short.

Keywords: impinging jets, acoustic heat transfer

1. Introduction

In order to transfer heat from a fire to the hot end of a regenerator in a thermoacoustic engine, without the complication of a tubular heat exchanger, a heated plate is arranged to radiate to the regenerator [1]. The hot end of the regenerator faces the plate across a cavity, with an exit to one side into a loop which communicates with the cold end of the regenerator, and acoustic waves are amplified in the regenerator. This works well initially, but once the acoustic intensity in the engine builds up, the plate is cooled substantially by the impingement of the acoustic flows. To quantify this process, data were sought for the heat transfer to an acoustically oscillating ‘jet’ impinging on a surface in an axisymmetric configuration.

When there is no mean flow, the oscillating flow is known as a 'synthetic jet' and there are a number of papers on the cooling of electronic equipment by this means, often with a recirculating flow within a disc-shaped cavity. The jet in these cases is narrow, and has a high velocity and a low frequency so that the stroke length L_0 is large, and the distance to the plate measured in jet diameters (H/D) is large. The present interest is in the opposite case, where H/D=0.1 and the effective stroke length is also very much smaller than the diameter, with the acoustic flow oscillating radially under a lip (see Fig. 1).

A series of papers by a group at Trinity College, Dublin, addresses this configuration and the literature is nicely reviewed by Persoons et al. [2]. However, their work [2,3] concerns $H/D \geq 2$ and $L_0/D > 1$ and is focussed on the generation of vortices around the jet, which does not occur for $L_0/D < 0.5$, according to Holman et al. [4]. For varying H/D, Chaudhari et al. [5] examined the average heat transfer to a target plate that was larger than the jet and found a strong dependence of the maximum heat flux (at H/D=6) on the Reynolds number ($Re^{1.25}$) for a fixed stroke length (L_0/D=13.75), but again this result is not directly relevant to our arrangement.

In the situation considered here, the acoustic displacements are very much less than the radius of the jet and there is no time for the laminar boundary layer to develop. The thermal penetration depth, $\delta_k = \sqrt{\alpha/\pi f}$, where α is the thermal diffusivity, is considerably less than the r.m.s. displacement $\xi \equiv u/2\pi f$, where u is the r.m.s. acoustic velocity. The equivalent stroke length is $L_0 = 2\sqrt{2}\xi$. This situation is more akin to that of hot plates transferring heat under acoustic oscillations of the gas over them to in-line cold plates. Shi et al. [6] plot the time-resolved temperature profiles for this geometry with a fixed frequency of 13.1 Hz, so that δ_k is 1.2 mm and $L_0/\delta_k \approx$ 50-100. They show that the cycle-averaged heat flux increases with Re (and hence with the displacements, at least up to the limit of their data) in spite of the displacement amplitude exceeding the plate lengths.

In the absence of really pertinent data in the literature for the impinging acoustic field, spatial distributions of time-averaged heat flux from a constant temperature plate have been measured for three different frequencies over a range of acoustic amplitudes.

2. Apparatus

The apparatus is shown in Fig. 1. It consists of a flat heated plate which can be moved horizontally and vertically beneath a large vertical duct. The duct is suspended from a loudspeaker enclosure which is used to excite the column of air in the duct. A sensor is embedded in the surface of the plate to measure the heat flux between the air jet and the plate. The whole apparatus is surrounded by plastic sheeting to prevent draughts from interfering with the measurements.

The loudspeaker enclosure contains a pair of Baseface SPL 12.1 'sub-woofer' loudspeakers facing one another and driven in parallel. These are powered by a 4000W power amplifier with a sinusoidal input signal. The input frequency and signal strength can be set manually but the measured audio power output is liable to drift by ± 3% for a fixed input. This arrangement produces a uniaxial plane wave excitation at the exit from the duct.

The duct is constructed from stainless steel cylinders and is 800 mm long and 300 mm in diameter (D). In order to replicate the geometry of the thermoacoustic engine, a regenerator stack is placed 20 mm above the duct exit. This consists of multiple layers of compressed fine wire mesh discs which completely fill the duct, totalling about 20 mm in thickness. Below the regenerator, a generic K-type thermocouple is positioned at the centre of the jet exit to measure the air temperature.

The duct has a vertical series of tapping holes, to which G.R.A.S. type 26AC microphones can be fitted. A spectrum analyser determines the output voltage from each microphone and the phase difference between them. The analyser also provides the input signal for the power amplifier.

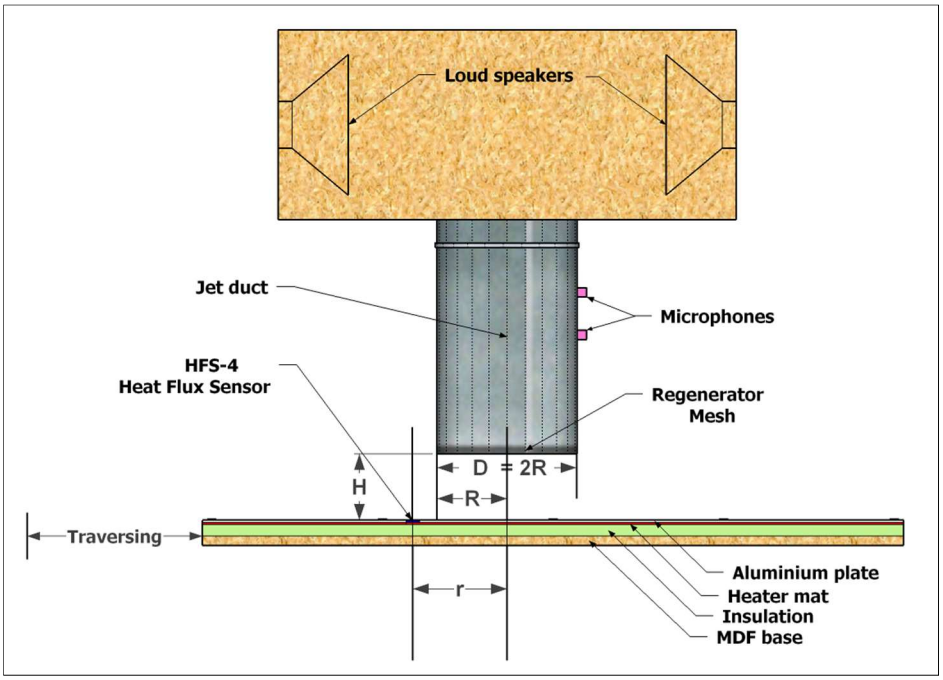

Figure 1. The apparatus and frame of reference

The impingement surface consists of a flat sheet of aluminium 5 mm thick and measuring 900 mm wide by 1500 mm along the main axis. The central strip 200 mm wide and 750 mm long is heated electrically from below by adhesive silicone heating mats. A 25 mm layer of polyisocyanurate is placed underneath to reduce heat losses from the underside. This is supported by a sheet of MDF as a base. This 'sandwich' is held together by countersunk bolts and forms a single component, which can be moved along the main axis back and forth below the duct.

A generic K-type thermocouple is placed at the centre of each heating mat. The thermocouples are used as input to five RF-100 temperature controllers These allow the heater mats to be kept at a steady temperature using a 4 second on-off heating cycle. If the heater mats are set to maintain a temperature of 60 degC under the plate then the top surface will be maintained at 57.7 ± 0.2 degC under natural convection conditions. The top surface approximates to a uniform wall temperature boundary on the path between the centre of the jet and the heat flux sensor.

An HFS-4 thin film heat flux sensor, 250 μm thick and supplied by Omega Engineering Inc., is embedded in the top surface of the aluminium plate on the main axis. The sensor consists of a thin polyamide film measuring 29 mm x 35 mm with an array of 56 thermocouples on each side. The voltage difference between the two sides of the film is proportional to the heat flux. The sensor was calibrated after manufacture and stated to generate 2.0 $\mu V/W/m^2$, with an accuracy of ± 10%. The sensor also incorporates a generic K-type thermocouple on the top surface.

The plate to duct spacing H = 30 mm. Further details have been given by Robinson in [7].

3. Experimental procedure

Heat flux, temperature and microphone readings were taken at 10 mm intervals as the heat sensor was moved from the stagnation position, with the sensor under the axis of the duct, to a position where the sensor was two duct radii from the centre. At each measurement position the apparatus was left to reach thermal equilibrium, and the two microphone signals were recorded. The microphone positions were then reversed and the readings repeated to eliminate any systematic bias in calculating the acoustic velocity by the two-microphone technique.

Thermocouple readings were taken from the centre of the air jet and at the surface of the heat flux sensor. The raw data were filtered to eliminate voltage spikes induced by the heating mat controllers. Both the heat flux and temperature data were averaged over a 4 second period to match a

complete cycle of the heater mats. Finally the trace from the heat flux sensor was averaged by eye. Typically it had a variability of ± 3%, but under the rim of the duct this variability rose to ± 10%. The error in assessing the average reading was nevertheless estimated to be less than 1%.

In studies with a constant impinging flow, the Nusselt number is calculated from the temperature difference between the plate and the air at the jet exit. However, in order to calculate a translatable Nusselt number in the presence of the oscillations, an estimate of the local bulk air temperature over the whole plate needs to be made. Clearly, at the outer limits of air movement caused by the jet, the air is at ambient temperature, but it is unclear how far under the jet this colder air penetrates. A judgement was made to use the measured air temperature everywhere inside the jet, and the measured ambient outside it, even though this necessarily gives rise to a discontinuity in *Nu*.

4. Results

The values for local heat flux have been converted to a Nusselt number based on the diameter of the jet, the thermal conductivity of the gas at the temperature of jet exit, and the temperature difference described above, where T_L is the local bulk gas temperature:

$$Nu \equiv \frac{\dot{q}''}{(T_w - T_L)} \frac{D}{k_0}$$

For this fixed geometry, the results can be analysed for their dependence on two independent parameters: the acoustic velocity at exit from the jet, and the frequency of excitation. The corresponding non-dimensional parameters are the Reynolds number, $\equiv uD/\nu$, where u is the r.m.s. acoustic velocity at jet exit, and the acoustic Reynolds number, $Re_\omega \equiv 2\pi f D^2/\nu$.

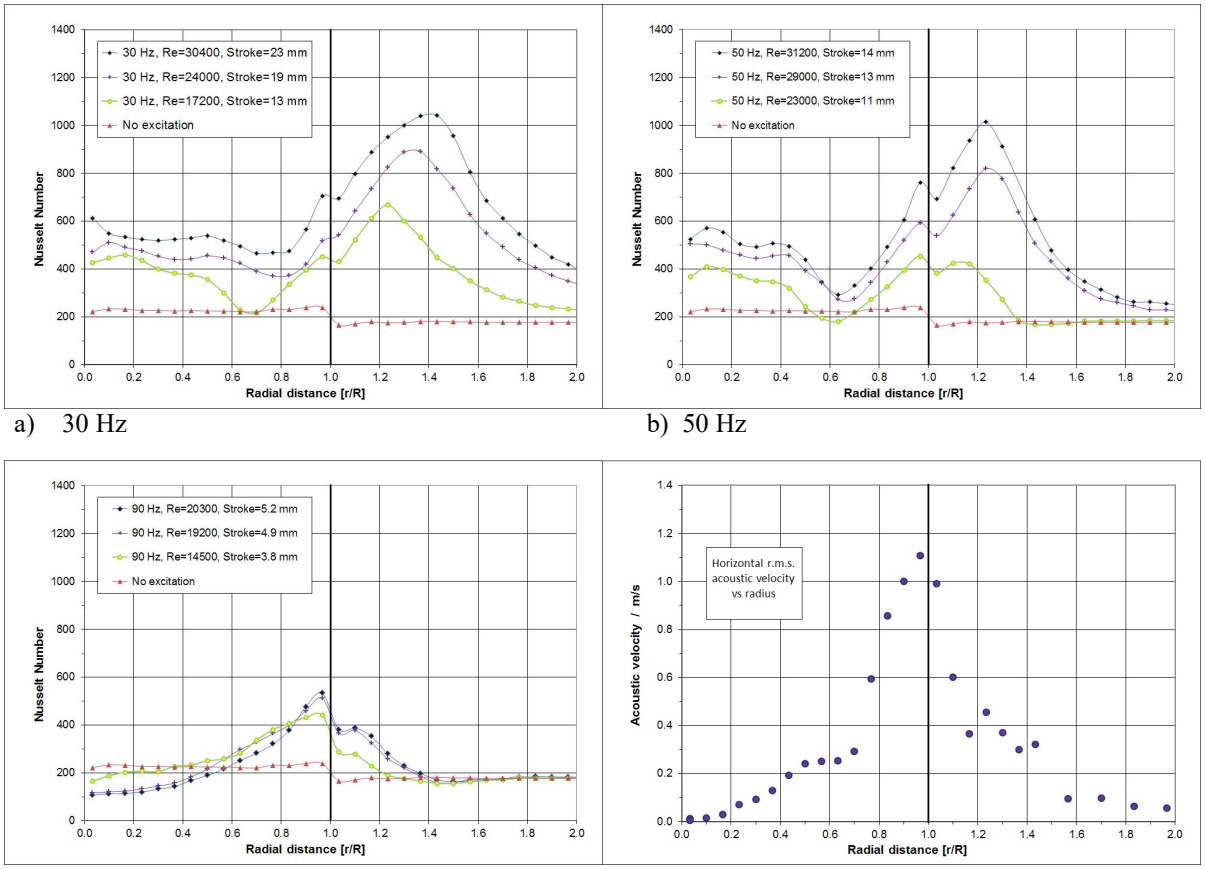

a) 30 Hz b) 50 Hz

c) 90 Hz d) 20 Hz

Figure 2. a) to c) Profiles of Nusselt number for three frequencies and various intensities of excitation with H/D=0.10. d) Approximate profile of r.m.s. acoustic velocity within 1 mm of the plate surface with H/D =0.13 (from Robinson [7]).

Alternatively, the velocity and frequency may be combined to yield the stroke length at the jet exit, and this used together with either velocity or frequency. Considering the physics of the acoustic flows driving the laminar boundary layer through which heat must be transferred (see the Introduction), the stroke length may be a more crucial parameter than the velocity per se, but it is difficult to achieve common values of stroke length over a wide range of frequencies. Since the thermal penetration depth is a function of the frequency, this parameter provides an alternative to the acoustic Reynolds number as a means of representing the frequency: $D/\delta_k = \sqrt{Re_\omega Pr/2}$, where Pr is the Prandtl number. This is also known as the Womersley number.

Fig. 2 displays the radial profiles of Nu for the three frequencies. The heat transfer without any acoustic excitation, by natural convection and radiation, is also shown. The intensity of excitation is here represented by the Reynolds number. Noteworthy features of these plots are:

a) The relative uniformity of the natural convection background across the plate.
b) The peaking of the heat transfer outside the radius of the jet, with the peak moving inwards progressively from $r = 1.4R$ at 30 Hz to $1.2R$ at 50 Hz and to 1.0 R at 90 Hz, where $R = D/2$.
c) A peak level at the two lower frequencies of five times the natural convection background.
d) The reduction of the heat transfer to the natural convection level at $r = 0.6$R at 30 Hz and 50 Hz, and to below this level for $r < 0.6$R at the higher acoustic intensities at 90 Hz.
e) The enhancement of heat transfer for up to a radius beyond the jet.

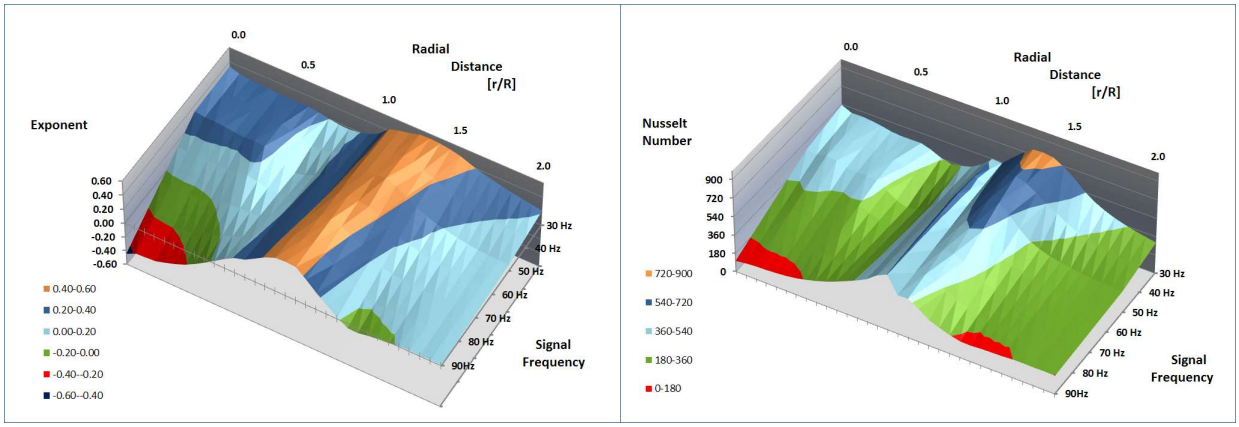

Figure 3. a) The exponent of apparent velocity dependence, interpolated between frequencies of 30 Hz, 50 Hz and 90 Hz. and b) the distribution of Nusselt number at velocity of 1.1 m/s (Re=21500)

As a means of interpolating and modestly extrapolating the data for each frequency, the Nusselt number for each point, including the natural convection value, was correlated by $Nu \propto Re^n$. Since it is clear that this relationship does not hold as Re goes to zero and natural convection dominates, the value of n (shown in Fig. 3a) is only an apparent exponent, and it actually becomes negative for small radii at 90 Hz, as shown above. However, the correlations enable the Nu values to be smoothed and compared at a common jet exit velocity (1.1 m/s) and the result is also shown in Fig. 3b. The two plots have a similar shape because n is a measure of the level as well as the velocity dependence of Nu. Clearly Nu falls with frequency at all radii. A qualitatively similar plot is obtained if comparison is made at a common displacement length, but in this case, the extrapolations involved in predicting the heat transfer at 90 Hz with displacements comparable to those at 30 Hz and 50 Hz are too large to be accurate.

Closer correlations are obtained at 30 Hz and 50 Hz and higher intensities by a relationship that is linear with u and that ignores the zero (natural convection) point. However, this linearity is far from perfect, and does not appear at 90 Hz inside the jet radius when the heat transfer is low and may be less than in natural convection (Fig. 4c).

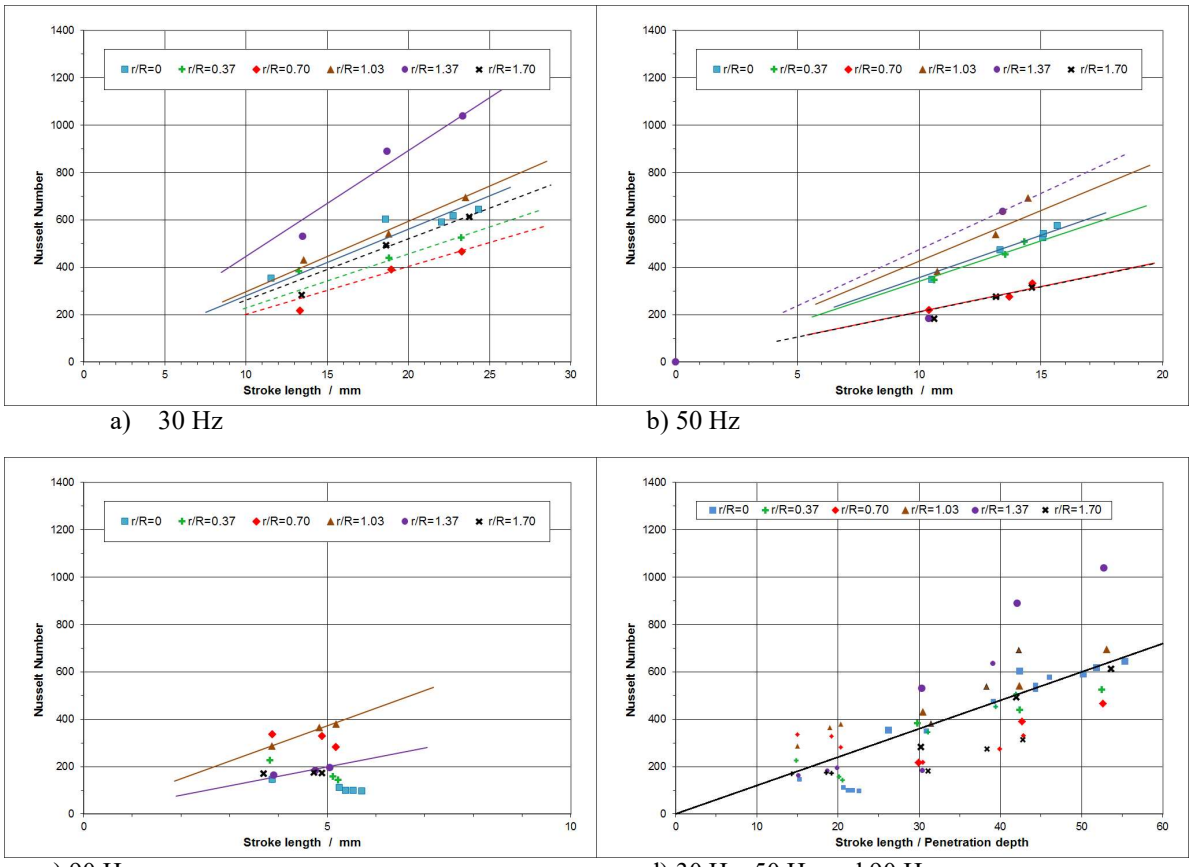

a) 30 Hz b) 50 Hz

c) 90 Hz d) 30 Hz, 50 Hz and 90 Hz

Figure 4. a) to c) Nusselt number as a function of the vertical stroke length for various radial positions. (The stroke length is proportional to the velocity for a given frequency.) d) Nusselt number as a function of the ratio of vertical stroke length to thermal penetration depth.

5. Discussion

The measured level of natural convection and radiation was remarkably uniform across the plate at *Nu*=220-230 inside the jet, and 166-180 outside it. A summary of correlations in the literature for the heat transfer from a flat plate of the dimensions used here [8] and a temperature difference from the surroundings of 30 degC, yields a Nusselt number of 144. However, if radiation to the body of the jet in the range *Nu*=10 to 30 is added, corresponding to an emissivity for the commercial aluminium plate of 0.1 to 0.3, then a total in the range 154 to 174 is estimated, agreeing with that measured outside the radius of the jet.

Inside the radius, the flow pattern was probably that shown in the schematic of Fig. 5a, with cold air from the edge of the plate drawn in along it to be heated and then rising under buoyancy to the cool surface of the mesh in the jet. The distributions in Fig. 2 for the four cases with acoustic excitation giving $Re > 23000$ ($u > 1.2$ m/s) show enhancement of the heat transfer under the jet by a factor of at least two, and just outside the jet by a factor of five.

In order to understand these distributions of heat transfer, it is necessary to postulate the likely velocity patterns close to the surface of the plate. Rectified measurements of the fluctuating signal from a hot-wire anemometer have been made in a similar configuration (but with a 38 mm gap to the plate) at 20 Hz by Robinson [7]. The hot-wire was positioned 1 mm from the plate, thus eliminating the vertical component of velocity but probably incurring calibration errors through heat loss to the plate. Nevertheless, the distribution of the r.m.s. signal (Fig. 2d) is indicative of the acoustic amplitude and this shows a very pronounced peak under the lip of the jet at r/R =1.0, with less than 25% of the peak for $r/R<0.6$ and $r/R>1.5$.

This observation, continuity considerations, and inviscid flow behaviour suggests that the acoustic flow distributions are as shown in the schematic of Figs. 5b and 5c. The outflow condition (Fig. 5b) involves a progressive increase of the horizontal mass flow in proportion to r^2, through annular sections of reducing height but increasing radius. Fig. 2d appears to show an r^2 dependence of the velocity along the plate, possibly because the effective flow area is nearly constant. For H/D<0.25, the flow must accelerate through the gap, as measured and calculated by Scholtz and Trass [9], and for H/D = 0.1, as here, the mean velocity is more than 2.5 times that at jet exit. Within the jet, any turbulence will be small-scale, generated by the passages of the fine mesh at exit, and there will be little mixing.

The acceleration will enhance the heat (or mass) transfer, but the theoretical prediction of Scholtz and Trass [9] from a viscous boundary layer calculation for steady outflow is that with H/D=0.05, the peak Sherwood number at r/R =1.0 is only twice that at the stagnation point (r=0). With H/D=0.10, Lytle and Webb [10] did indeed measure a mean velocity in the gap of more than twice that at jet exit. They also measured a peak Nusselt number of twice that at the stagnation point with Re = 23000, but surprisingly this peak was as far out as r/R=2.5. It was associated with a peak in the turbulence profile as the flow expanded in a wall jet, promoting mixing in the shear layer. This element is relevant to the oscillating case, but the Nusselt number had the $Nu \propto Re^{0.5}$dependence associated with growth of a boundary layer from the stagnation point, and this is not relevant to our unsteady cases.

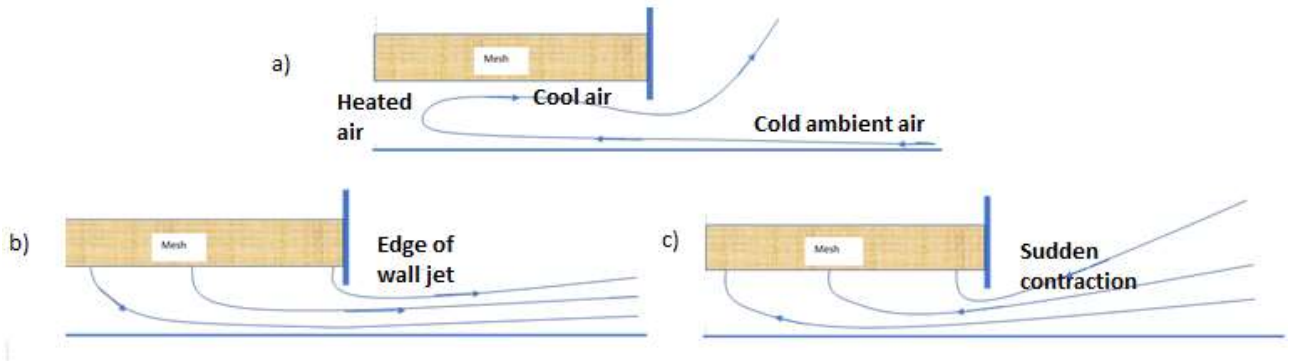

Figure 5. Expected flow patterns for a) no excitation, and b) and c) two phases of excitation.

With inflow (Fig. 5c), the air will be drawn from a larger surrounding area and impinge on the plate before distributing itself uniformly across the mesh. No guidance from the literature is available but, in this phase of the cycle, the distribution of velocity close to the plate will be very different from that in outflow, and there will be a vena contracta and the maximum velocity inside the jet region. Thus from quasi-steady considerations of the maximum velocity at the two extreme conditions, the position of maximum cycle-averaged heat transfer just outside the lip (r/R =1.0 to 1.4) is likely to be due to the balance of the two very different heat transfer profiles, although neither will be described by the steady conditions.

This is because the thermal penetration depth $\delta_k = \sqrt{\alpha/\pi f}$, is only about 0.5 mm for 30 Hz, whereas the maximum horizontal stroke length is estimated to vary from about 15 mm at r/R=0.5 to 60 mm at the gap. The quasi-steady viscous and thermal boundary layers are of little relevance and it should not be expected that $Nu \propto Re^{0.5}$. The linearity with Re that is observed in Fig. 2 is due to the related increase in stroke length, rather than in velocity directly. With greater than about 30 mm horizontal strokes, cold air is drawn down onto the surface of the plate from positions close to the jet exit in one half of the cycle and from the surroundings in the other half, giving rise to very high heat transfer close to the lip.

For 90 Hz, the maximum horizontal strokes fall to 4 mm at r/R=0.5 and 15 mm at the gap, and about half of these values at the lowest acoustic intensity, while the thermal penetration depth is only reduced to 0.3 mm. The ratio L_0/δ_k is proposed as the parameter that characterises the heat transfer at a given radial location (although the local horizontal stroke might be better if accurate

data were available). The Nusselt number is linearly related to this parameter, bringing all three frequencies into line (Fig. 4d), until the excitation is too weak to suppress natural convection effects, when $Nu < 300$. Thus the heat transfer is found to be linearly related to the acoustic velocity and to the square root of the frequency.

With progressively shorter strokes, the acoustic enhancement of the heat transfer at $r/R = 0.6$ to 0.7 is eliminated, while with the much shorter strokes at $f = 90$ Hz, there is actually suppression of the natural convection contribution. These observations suggest that the flow pattern in Fig. (5a) is prevented by the radially coherent oscillations associated with the small displacement acoustic waves but that these are not able to replace the contribution to heat transfer because they do not mix the gas in the cavity sufficiently on the large scale for the temperature close to the plate to be held down.

Outside the diameter of the jet, there is a radial wall jet with rapid deceleration of the flow which generates high turbulence in the outflow. This alternates with low turbulence inflow. Heat transfer drops off rapidly with radial distance in both phases, so the average Nusselt number does so also, particularly with the short acoustic displacements at 90 Hz.

6. Conclusions

The local heat transfer from a constant temperature plate under an impinging acoustic jet positioned close to the surface has been measured for varying acoustic velocities and frequencies. At moderate and high acoustic intensities, the radial distributions show enhancements over the natural convection and radiation background by a factor of two on the axis and by as much as five close to the lip of the jet. Outside the radius of the jet, the acoustic enhancement falls off within a radius. At lower intensities, the acoustic contribution appears to be sufficient to suppress the natural convection, while not making as big a contribution to heat transfer, so that the net heat transfer is actually reduced.

Before this point is reached, the Nusselt number has been shown to be proportional to the acoustic velocity and the square root of the frequency, suggesting the ratio of the stroke length to the thermal penetration depth as the appropriate parameter for correlation of the results at each radial position.

References

1. Lawn, C.J. Development of a thermoacoustic travelling-wave engine, *Proc. IMechE, Part A., J.Power and Energy,* 227(7)(2013) 783-802.
2. Persoons, T., McGuinn, A., and Murray, D.B. A general correlation for the stagnation point Nusselt number of an axisymmetric impinging synthetic jet, *Int. J. Heat Mass Transfer,* 54 (2011) 3900-3908.
3. Valiogue, P., Persoons, T, McGuinn, A. and Murray, D.B. Heat transfer mechanisms in an impinging synthetic jet for a small jet-to-surface spacing, *Experimental Thermal and Fluid Science,* 33 (2009) 597-603.
4. Holman, R., Utturkar, Y., Mittal, R.,Smith ,B. and Cattafesta, L. Formation criteria for synthetic jets, *AIAA J.,* 43 (10) (2005) 2110-2116.
5. Chaudhari, M., Puranik, B. and Agrawal, A. Heat transfer characteristics of synthetic jet impingement cooling, *Int. J. Heat and Mass Transfer,* 53 (2010) 1057-1069.
6. Shi, L., Mao, X. and Jaworski, A.J. Application of planar laser-induced fluorescence measurement techniques to study the heat transfer characteristics of parallel-plate heat exchangers in thermoacoustic devices. *Meas. Sci. Technol.* 21(2010) 115405.
7. Robinson, N.J.M. The enhancement of heat transfer by acoustic gas flows. Master of Science Thesis, Queen Mary University of London, Sept 2013.
8. Corcione, M. Heat transfer correlations for free convection from upward facing horizontal rectangular surfaces. *WSEAS Transactions on Heat and Mass Transfer, 2007.*
9. Scholtz, M.T. and Tross, O. Mass transfer in a nonuniform impinging jet. *AIChE J.* 16(1) (1970) 82-96.
10. Lytle, D. and Webb, B.W. Air jet impingement heat transfer at low nozzle-plate spacings. *Int. J. Heat Mass Transfer,* 37 (12) (1994) 1687-1697.